

ISSN 0280-5316
ISRN LUTFD2/TFRT--5494--SE

Minimum Energy Control Applied to Mechanical Systems Driven by Induction Motors

Mikael Petersson

Department of Automatic Control
Lund Institute of Technology
December 1993

*Laboratoire d'Automatique
de Grenoble*

Unité de Recherche Associée au CNRS 228

ISSN 0280-5316

ISRN LUTFD2/TFRT--5494--SE

Minimum Energy Control Applied to Mechanical Systems Driven by Induction Motors

Mikael Petersson

Laboratoire d'Automatique de Grenoble

Department of Automatic Control Lund Institute of Technology P.O. Box 118 S-221 00 Lund Sweden		<i>Document name</i> MASTER THESIS	
		<i>Date of issue</i> December 1993	
		<i>Document Number</i> ISRN LUTFD2/TFRT--5494--SE	
<i>Author(s)</i> Mikael Petersson		<i>Supervisor</i> C. Canudas de Wit, S.I. Seleme, R. Johansson	
		<i>Sponsoring organisation</i>	
<i>Title and subtitle</i> Minimum Energy Control Applied to Mechanical Systems Driven by Introduction Motors.			
<i>Abstract</i> <p>We shall present innovative approach for the torque tracking control of induction motors based on the minimization of the energy. A nonlinear schema is proposed which inherits both the performance features of nonlinear Euler-Lagrange based Schemes (needed for fast dynamical systems) and the power efficiency features of the minimum energy approach. This study concerns the case of time varying reference trajectories. The design is proceeded as follows. First, the study of the optimization problem of the reference states which minimize the machine's magnetic energy. Second, the design of a nonlinear feedback control which renders invariant this minimum energy operation manifold. Finally, a comprehensive simulation section showing both, the performance characteristics and the efficiency improvement of our scheme.</p>			
<i>Key words</i> Nonlinear control, Induction motors, Variational problem, Dynamic programming, Euler-Lagrange systems			
<i>Classification system and/or index terms (if any)</i>			
<i>Supplementary bibliographical information</i>			
<i>ISSN and key title</i> 0280-5316		<i>ISBN</i>	
<i>Language</i> English	<i>Number of pages</i> 38	<i>Recipient's notes</i>	
<i>Security classification</i>			

Contents

1	Introduction	3
2	Problem Formulation	5
3	The Dynamical Model	6
3.1	The Nominal Motor Model	6
3.2	The Mechanical Model	8
3.3	Physical Properties	8
4	The Minimum Energy Approach	10
5	The Reference Model	13
5.1	Derivation of a State Representation	13
5.2	Constant Rotor Flux Model	16
6	Optimization	17
6.1	Problem Formulation	17
6.2	The Existence of Solution	19
6.3	Dynamic Programming	20
6.4	Numerical Solution	21
7	Control	24
7.1	Stability Analysis	24
7.2	The Control Law	27
8	Simulation Results	29
9	Conclusion	34
A	Notations	35
	Bibliography	36

Chapter 1

Introduction

Induction motor drives present very interesting physical characteristics. They are robust, capable of delivering torques of up to twice the nominal rate (for short endurance) and present a quite large range of speed. A slight drawback is that the generated torque is not uniquely defined due to nonlinearity, which makes the control design more difficult. The interest in these machines has grown after the successful appearance of the field oriented control [1, 8]. There is now a lot of research done in order to obtain more accurate and performing applications.

Due to its characteristics and the nature of torque control like applications (robotics, machine tools, roller mills, etc), the driver operates mostly below its rated power. The idea of fluxing the machine at its nominal rate is far from being the best in terms of efficiency, when the demanded torque is inferior to the machine's rated value [14].

Considering the growing interest of induction motor drives for applications where performance and efficiency are demanded [8, 9, 10] the minimization of the energy related to control is an interesting problem. Recently, an approach for the torque regulation of induction motors by minimizing an energy cost function (the magnetic energy) was developed, [4, 14]. This approach gives minimum energy at steady-state operation under torque regulation. For a given constant torque, this implies minimum reactive power, on one hand, and a good trade-off between minimum current and maximum efficiency, on the other. The natural extension of this problem is to treat the case of time-varying torque references.

The aim of this study is to design an optimal control, in the sense of energy, where, for all time t , optimum-energy state trajectory are attained. The problems will be treated separately: on one hand the mechanical system and its optimum torque feedback; on the other hand the induction motor drives and the optimization of reference states for a minimum magnetic energy profile. Then, we will address the control problem of the two coupled systems.

The optimum feedback which minimizes velocity and positional errors, that is, the minimum torque $\tau(t)$ that minimizes the tracking errors for the mechanical system is considered as the output signal to be tracked. The problem of deriving optimal torque reference has already been addressed in [6, 7]. Our main concern

here is to perform the optimal (or any other) torque signal tracking with minimum magnetic energy for the motor. This will be carried out in parts.

In Chapter 5, we proceed the derivation of reference state vector (the energy shaping manifolds) which imbed the torque tracking constraint and fulfills the dynamical constraints posed by the motor model. In other words, a set of manifolds described by the time varying reference states will be derived, in order to make it possible to, in Chapter 7, solve the feedback control problem.

As it will be seen later on, there is a degree of freedom in the choice of the reference states which will be exploited to minimize the electro-magnetic energy of the motor. This will be addressed in Chapter 6, as a typical weak extremum variational problem and solved using dynamic programming.

Chapter 7 will deal with the "energy shaping" problem. By that we understand the control scheme which renders invariant the optimal energy reference manifold. This will be done using Lyapunov's theory.

Chapter 8 will present some simulation results of the optimal energy torque tracking approach and Chapter 9 will summarize the results of this study.

Chapter 2

Problem Formulation

One of the main purposes of this study is to find a reference state trajectory which minimizes the magnetic energy of the induction motor, or a function thereof, during torque regulation. The motor is normally described by six differential equations for the electro-magnetic part, and one differential equation for the mechanical motion. Using the Park transformation these are reduced to a set of five.

Moreover, a nominal motor model will be considered which is presented in Chapter 3 under the assumptions of

- A.1** The motor model is exactly known with constant parameters and all its states measurable.
- A.2** The desired torque is twice differentiable and uniformly bounded.
- A.3** The mechanical speed is available.
- A.4** The load torque is known.

The objective in the controller design is that the motor state asymptotically attains the reference state, or in other words, the output torque shall converge to the desired one.

Formulating this as a mathematical problem corresponds to an optimization of an expression of the energy subject to differential and nonlinear constraints.

Chapter 3

The Dynamical Model

In this section a model of the induction motor driving some mechanical system is presented. This model emphasizes the physical structure and in particular the energy dissipative properties [11]. A well known fact is that there is a coupling between the motor drive and the mechanical system, see for example [11] and references therein.

The electro-mechanical system can be seen either as a single bilinear system described by the complete state vector (motor currents and mechanical velocity) or as two separate subsystems in feedback connection. In such case the electrical torque delivered by the motor is considered as the input to the driven mechanical system, while the rotor speed, which is a state of the latter system, can be regarded as an input to the induction motor.

3.1 The Nominal Motor Model

The induction motor presents a somewhat involved theory since it has rotating magnetic fields. Hence, a reduced mathematical model will be used, which incorporates most of the qualitative features of an actual motor. It is described in terms of the total energy function (the magnetic energy) and generalized forces, using the Lagrange formulation [12]. The dq reference frame used (Fig 3.1) turns with the primary frequency, ω_a , which is one of the control inputs.

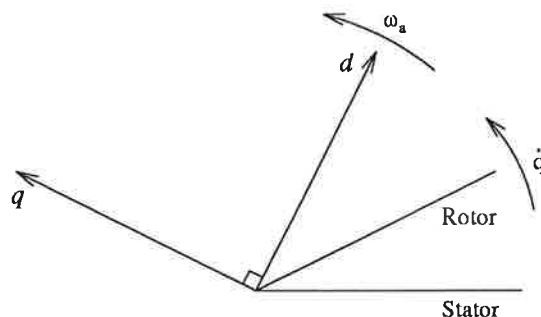


Figure 3.1: The rotating dq frame.

The rotor, and thus the shaft, turns with the angular speed \dot{q} , while the stator is fixed by nature. The exact position of the coordinate frame, or rather the relative velocity with respect to the rotor speed, will be decided further on.

The classical dq induction motor model in consideration is described by

$$D\dot{\mathbf{x}} + [N(\mathbf{u}_3, \dot{q}) + R]\mathbf{x} - n(\mathbf{x})\dot{q} = M \begin{bmatrix} u_1 \\ u_2 \end{bmatrix} \quad (3.1)$$

$$\begin{aligned} \tau(\mathbf{x}) &= vL_{sr}(\mathbf{x}_2\mathbf{x}_3 - \mathbf{x}_1\mathbf{x}_4) = -n^T(\mathbf{x})\mathbf{x} \\ n(\mathbf{x}) &= v[(L_s\mathbf{x}_2 + L_{sr}\mathbf{x}_4) \quad -(L_s\mathbf{x}_1 + L_{sr}\mathbf{x}_3) \quad 0 \quad 0]^T \end{aligned} \quad (3.2)$$

where v is the number of pole pairs,

$$\mathbf{x} = [\mathbf{x}_1 \quad \dots \quad \mathbf{x}_4]^T \stackrel{def}{=} [i_s^d \quad i_s^q \quad i_r^d \quad i_r^q]^T$$

stand for the stator and rotor currents in the dq coordinate frame and the control input vector

$$\mathbf{u} = [u_1 \quad u_2 \quad u_3]^T \stackrel{def}{=} [V_s^d \quad V_s^q \quad \omega_a]^T$$

is composed by the stator voltages and the primary frequency, respectively. The (4×4) matrices, D , N and R , and the (4×2) matrix M are defined by:

$$\begin{aligned} D &\stackrel{def}{=} \begin{bmatrix} L_s \mathcal{I}_2 & L_{sr} \mathcal{I}_2 \\ L_{sr} \mathcal{I}_2 & L_r \mathcal{I}_2 \end{bmatrix} \\ N &\stackrel{def}{=} \begin{bmatrix} L_s \mathcal{J}_2 & L_{sr} \mathcal{J}_2 \\ L_{sr} \mathcal{J}_2 & L_r \mathcal{J}_2 \end{bmatrix} (\mathbf{u}_3 - v\dot{q}) \\ R &\stackrel{def}{=} \begin{bmatrix} R_s \mathcal{I}_2 & 0 \\ 0 & R_r \mathcal{I}_2 \end{bmatrix}; \quad M \stackrel{def}{=} \begin{bmatrix} \mathcal{I}_2 \\ 0 \end{bmatrix} \end{aligned}$$

where R_s and R_r are the stator and rotor resistances, L_s, L_r and L_{sr} are the stator, rotor and mutual inductances, respectively. \mathcal{I}_2 is the (2×2) identity matrix and \mathcal{J}_2 is the (2×2) skew-symmetric matrix

$$\mathcal{J}_2 \stackrel{def}{=} \begin{bmatrix} 0 & -1 \\ 1 & 0 \end{bmatrix} = -\mathcal{J}_2^T$$

It is worth mentioning that this energy based approach is invariant with respect to rotational transformations, a conclusion drawn by Espinosa and Ortega. This will also be seen in Chapter 4. Any other reference frame, obtained by a rotation or a linear transformation of the states, could be used as well (the stationary ab -frame model for instance).

3.2 The Mechanical Model

The rotational motion of the mechanical system is described by a first order differential equation for the speed, \dot{q} :

$$J\ddot{q} + b\dot{q} = \tau(\mathbf{x}) - \tau_L \quad (3.3)$$

where J , b and τ_L are the rotor inertia, the motor damping and the load torque, respectively.

3.3 Physical Properties

In modeling physical systems the underlying structure is exploited in a crucial way. Some dissipative properties, as eddy currents, are neglected and nonlinearities, as iron saturation, are not modeled due to complexity and uncertainty.

We can, from (3.1)-(3.2) and (3.3), see that the mechanical speed \dot{q} and the electrical torque $\tau(\mathbf{x})$ are the coupling elements of the two subsystems (the induction motor and the mechanical system).

The primary frequency, the third control variable, is as usual partitioned in two parts:

$$u_3 = v\dot{q} + \omega_s \quad (3.4)$$

where \dot{q} is the mechanical velocity and ω_s the auxiliary input variable named the slip frequency.

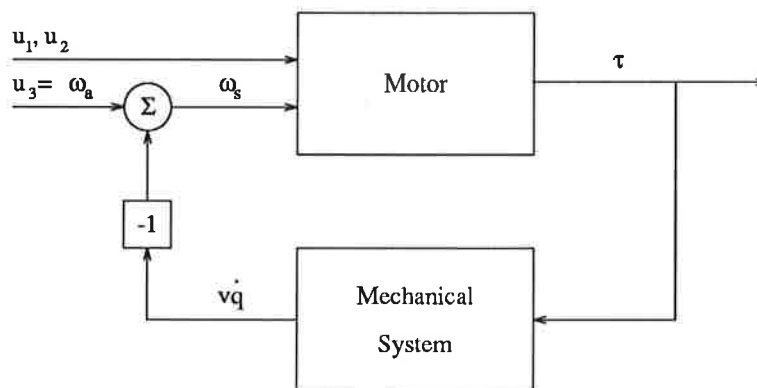


Figure 3.2: The induction motor and the mechanical system as a feedback connection of passive systems.

The nominal motor gets, in driving mode, its energy from the supply voltage and the consumed energy is the thermal losses and the conversion to mechanical energy. As a generator, the rotation of the rotor induces currents in the stator and therefore the energy conversion is reversible. Concerning the shaft, the losses come either as

load torque and friction or as the induction mentioned above and the driving forces are the output torque or the load torque.

Since the energy content of a physical body cannot be changed instantaneously, the rotational velocity of the shaft must always be a continuous function of time. This, and the knowledge of that the systems can not possess infinite energy, guarantee the boundedness and smoothness¹ of \dot{q} . This means that there is no finite escape time problem in the feedback connection of the motor and mechanical system.

In the system representation (3.1) has the workless forces been separated by the choice of N , which has the property

$$\mathbf{x}^T N \mathbf{x} \equiv 0, \forall \mathbf{x}$$

The terms $n(\mathbf{x})\dot{q}$ and $-n(\mathbf{x})^T \mathbf{x}$ can be seen as the force couplings between the magnetic and the mechanical systems. They are also workless as will be seen during the stability analysis in Chapter 7. The only dissipative force modeled is $R\mathbf{x}$, which represents the thermal losses in the conductors.

The magnetic fluxes in the motor is linearly related to the currents in the dq reference frame as

$$\begin{bmatrix} \phi_s^d \\ \phi_s^q \\ \phi_r^d \\ \phi_r^q \end{bmatrix} = D \mathbf{x} = \begin{bmatrix} L_s \mathcal{I}_2 & L_{sr} \mathcal{I}_2 \\ L_{sr} \mathcal{I}_2 & L_r \mathcal{I}_2 \end{bmatrix} \begin{bmatrix} i_s^d \\ i_s^q \\ i_r^d \\ i_r^q \end{bmatrix} \quad (3.5)$$

This dependency will be used later on to ease the coming design.

¹A function is in the following said to be smooth in an interval if it is continuous and has continuous derivative in this interval.

Chapter 4

The Minimum Energy Approach

Typical induction motors are designed to operate at their rated operating point with maximum efficiency and power factor. For operation away from these points there are some constraints to be respected in order to preserve the motor and its electrical power supply from overcharges. The power, or energy flow, in the electro-mechanical system has two components. These are the real power, or active energy flow, on the one hand and the reactive power on the other hand. The first is imposed by load and internal losses of the motor and the second is determined essentially by magnetic fluxes inside the machine.

The system Hamiltonian, which for the symmetric induction motor, coincides with the Lagrangian, can according to [4, 14], by neglecting the shaft compliance and the mechanical dissipation terms, be written as

$$\begin{aligned}\mathcal{H}(\mathbf{x}) &\stackrel{def}{=} \frac{1}{2} \mathbf{x}^T D \mathbf{x} \\ &= \frac{1}{2} (L_s (x_1^2 + x_2^2) + L_r (x_3^2 + x_4^2) + 2L_{sr} (x_1 x_3 + x_2 x_4))\end{aligned}\quad (4.1)$$

with $D = D^T > 0$ defined as in Chapter 3.

The Hamiltonian, $\mathcal{H}(\mathbf{x})$, represents the total magnetic energy in the machine and since the induction motor is seen as a consumer of reactive power, it is reasonable to minimize this quantity.

The state variables are expressed in the synchronous rotating dq reference frame, which turns with the angular velocity ω_a . It is possible to rewrite (4.1) as a function of the two-dimensional current vectors \vec{i}_s and \vec{i}_r , as

$$\mathcal{H}(\vec{i}_s, \vec{i}_r) = \frac{1}{2} L_s \langle \vec{i}_s | \vec{i}_s \rangle + \frac{1}{2} L_r \langle \vec{i}_r | \vec{i}_r \rangle + L_{sr} \langle \vec{i}_s | \vec{i}_r \rangle \quad (4.2)$$

where $\langle \cdot | \cdot \rangle$ denotes the scalar (inner) product of two vectors.

Additionally, this equation may be rewritten in terms of the magnitudes of the vectors and their intermediate angle δ :

$$\mathcal{H}(|\vec{i}_s|, |\vec{i}_r|, \delta) = \frac{1}{2} L_s |\vec{i}_s|^2 + \frac{1}{2} L_r |\vec{i}_r|^2 + L_{sr} |\vec{i}_s| |\vec{i}_r| \cos \delta \quad (4.3)$$

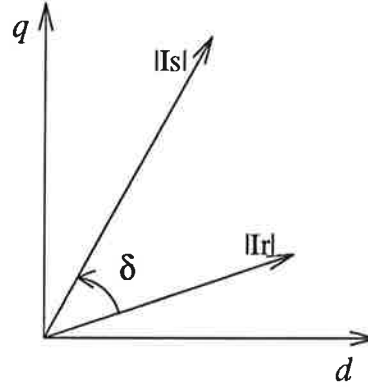


Figure 4.1: The stator and rotor currents in the dq frame.

We are also able to conclude the important fact that the magnetic energy is invariant with respect to the choice of reference frame, since it only depends on the amplitudes of the currents and the angle between them.

One has to keep in mind that the minimization has to be done subject to some control objective, as the torque tracking object which is used here. The torque function (3.2) can be expressed by the same quantities as used above, hence we rewrite it as

$$\tau(|\vec{i}_s|, |\vec{i}_r|, \delta) = v L_{sr} |\vec{i}_s| |\vec{i}_r| \sin \delta \quad (4.4)$$

where v as before is the number of pole-pairs.

The advantages of controlling the induction motor at minimum energy are basically related with its power factor. The active power, P_{act} , of the machine is the sum of the output power, P_{out} , and the internal losses, P_{loss} ,

$$P_{act} \stackrel{def}{=} P_{out} + P_{loss} \quad (4.5)$$

where

$$P_{out} \stackrel{def}{=} \dot{q} \tau(|\vec{i}_s|, |\vec{i}_r|, \delta) \quad (4.6)$$

According to [14], the reactive power, Q , can be written as

$$Q \stackrel{def}{=} \omega_a |\vec{\phi}_s| |\vec{i}_s| \cos \gamma \quad (4.7)$$

where ω_a is the primary frequency and γ denotes the angle between the stator current vector and the stator flux vector, $\vec{\phi}_s$.

Internal losses of the machine, P_{loss} , are given as the sum of the current-squared losses, P_{cu} and the core losses, P_{co} ,

$$P_{loss} \stackrel{def}{=} P_{cu} + P_{co} \quad (4.8)$$

The first ones, given in terms of the stator and rotor currents in the dq frame, are:

$$P_{cu} = 1.5(R_s |\vec{i}_s|^2 + R_r |\vec{i}_r|^2) \quad (4.9)$$

Core losses are composed of the Foucault current losses and the magnetic hysteresis losses in the iron core (stator and rotor). It is well known that for sinusoidally applied flux, within a limited-frequency range, core losses can be modeled, approximately, as a function of the excitation frequency and the air-gap flux, $\vec{\phi}$, as

$$P_{co} = 1.5(K_h\omega_a\vec{\phi}^2 + K_f\omega_a^2\vec{\phi}^2) \quad (4.10)$$

where K_h and K_f are coefficients for hysteresis and Foucault currents, respectively (see [10] and references therein).

The air-gap flux, under normal operation, can be approximated to,

$$\vec{\phi} = \frac{L_{sr}}{L_s}\vec{\phi}_s \quad (4.11)$$

Therefore, the total electrical losses of (4.8) can, by using 3.5, be expressed as a function of the states, \mathbf{x} and of the excitation frequency, ω_a .

$$\begin{aligned} P_{loss} = & 1.5\{[R_s + L_s L_{sr}(K_h\omega_a + K_f\omega_a^2)](x_1^2 + x_2^2) \\ & + [R_r + \frac{L_{sr}^3}{L_s}(K_h\omega_a + K_f\omega_a^2)](x_3^2 + x_4^2) \\ & + 2L_{sr}(K_h\omega_a + K_f\omega_a^2)(x_1x_3 + x_2x_4)\} \end{aligned} \quad (4.12)$$

The minimum energy criterion:

In [14] it was concluded that for almost all the range of speed of the machine *the minimum energy operation* corresponds to *the minimum reactive power*.

Even though minimization of the magnetic energy doesn't necessarily mean minimization of the internal losses (4.12), in the machine, the solutions of both problems are nearly the same, specially when at relatively high speed \dot{q} . This can be intuitively seen from the similarities between (4.1) and (4.12). On the other hand, the practical problem with specifically minimizing (4.12) is that it strongly depends on the knowledge of R_s and R_r , which can vary of up to 100%, and on the empirical values of K_h and K_f . This is not the case for the energy function (4.1) whose parameters, L_s , L_r and L_{sr} , are constant if the machine is not magnetically saturated and vary up to 30%, under saturation.

Chapter 5

The Reference Model

The present Chapter deals with the construction of a state reference model based on the nominal dynamical model of the induction motor. This model can be seen as a set of manifolds with some internal properties (to yield the energy shaping of the system in the feedback loop) which imbed the time varying output constraint. This means that the desired state, $x_d(t)$, should generate the desired torque trajectory, $\tau_d(t)$ for all time t . Our interest lies also in finding this reference state trajectory under the objective that field orientation should be obtained.

5.1 Derivation of a State Representation

In order to facilitate the forthcoming optimization, a feedforward time-varying state reference, denoted $x_d(t)$, shall now be established. The torque regulation objective is

$$\tau(x_d) - \tau_d(t) = 0 \quad (5.1)$$

The desired state, $x_d(t)$, shall also for any given torque curve, $\tau_d(t)$, fulfill the dynamic equation of the motor

$$D\dot{x}_d + [N(u_3, \dot{q}) + R]x_d - n(x_d)\dot{q} = M \begin{bmatrix} u_{d1} \\ u_{d2} \end{bmatrix} \quad (5.2)$$

where u_{d1} and u_{d2} denotes the desired input (see below). The third input, u_3 , is the degree of freedom to be used in the forthcoming optimization. A difficulty with the induction motor is that the torque is a nonlinear function of the state. One way to overcome this has been presented in the, nowadays classical, Field Oriented Control (FOC) [1, 8]. There, the induction motor was made to behave like an DC-motor where torque is proportional to the product of a current and a constant flux. Here, in contrary, we will allow the flux to be varying.

Considering constraints (3.1), posed by the induction motor model, and the fact that the matrix M is of full rank, the desired stator voltages will be given by the projection

$$\begin{bmatrix} u_{d1} \\ u_{d2} \end{bmatrix} = M^+ \{D\dot{x}_d + [N(u_3, \dot{q}) + R]x_d - n(x)\dot{q}\} \quad (5.3)$$

where the matrix M^+ is the pseudo inverse of M

$$M^+ \stackrel{\text{def}}{=} (M^T M)^{-1} M^T = \begin{bmatrix} \mathcal{I}_2 & 0 \end{bmatrix} \quad (5.4)$$

Substituting (5.3) into the motor equation (3.1), with $\mathbf{x} = \mathbf{x}_d$, gives

$$[\mathcal{I}_4 - M M^+] [D \dot{\mathbf{x}}_d + [N(u_3, \dot{q}) + R] \mathbf{x}_d - \eta(\mathbf{x}) \dot{q}] = 0$$

which is equivalent to the two following natural constraints

$$\begin{aligned} L_{sr} \dot{x}_{d1} + L_r \dot{x}_{d3} - (L_{sr} x_{d2} + L_r x_{d4})(u_3 - v \dot{q}) + R_r x_{d3} &= 0 \\ L_{sr} \dot{x}_{d2} + L_r \dot{x}_{d4} + (L_{sr} x_{d1} + L_r x_{d3})(u_3 - v \dot{q}) + R_r x_{d4} &= 0 \end{aligned} \quad (5.5)$$

Further, a field oriented objective is introduced. In other words, the q component of the rotor flux will always, in the considered control reference frame, fulfill

$$\phi_r^q = L_{sr} x_{d2} + L_r x_{d4} \equiv 0 \quad (5.6)$$

which will somewhat reduce (5.5). The difference from the FOC approach is that the remaining part of the rotor flux is not held constant.

The set of condition that the state reference is submitted to, can now, using the slip frequency relation (3.4), be written as

$$L_{sr} \dot{x}_{d1} + L_r \dot{x}_{d3} + R_r x_{d3} = 0 \quad (5.7)$$

$$(L_{sr} x_{d1} + L_r x_{d3}) \omega_s + R_r x_{d4} = 0 \quad (5.8)$$

$$L_{sr} x_{d2} + L_r x_{d4} = 0 \quad (5.9)$$

$$v L_{sr} (x_{d2} x_{d3} - x_{d1} x_{d4}) - \tau_d(t) = 0 \quad (5.10)$$

The first two equations stem from (5.5) using (5.6) and the last is the torque regulation constraint (5.1).

By manipulating (5.8)-(5.10) the fourth reference state is obtained as

$$x_{d4}^2 = \frac{1}{v R_r} \omega_s(t) \tau_d(t) \quad (5.11)$$

Since the sign of the slip frequency, by nature, is the same as that of the torque,

$$\text{sgn}(\omega_s) = \text{sgn}(\tau_d)$$

This stems from the physics of the motor. Therefore the quantity (5.11) is always positive.

The slip frequency being positive implies positive torque (motor action) and, vice versa, negative slip frequency corresponds to negative torque (generator action). Furthermore, zero slip frequency implies a zero torque since there is no rotor induction (rotor flux and currents are zero).

We will take the positive square root of (5.11) as the fourth reference state. If the negative root had been chosen instead we would obtain a revolution of the currents in the reference frame, but it would not have affected the forthcoming results.

Equations (5.7) and (5.8) gives the third state as a function of the fourth and its derivative. Then (5.8) and (5.9) yield the first and the second state, respectively.

The solution is¹

$$\begin{aligned} x_{d1} &= -\frac{1}{L_{sr}} \left[\frac{L_r}{\sqrt{R_r v}} \frac{d}{dt} \left[\sqrt{\frac{\tau_d}{\omega_s}} \right] + \sqrt{\frac{R_r}{v}} \sqrt{\frac{\tau_d}{\omega_s}} \right] \\ x_{d2} &= -\frac{L_r}{L_{sr} \sqrt{R_r v}} \sqrt{\tau_d \omega_s} \\ x_{d3} &= \frac{1}{\sqrt{R_r v}} \frac{d}{dt} \left[\sqrt{\frac{\tau_d}{\omega_s}} \right] \\ x_{d4} &= \frac{1}{\sqrt{R_r v}} \sqrt{\tau_d \omega_s} \end{aligned} \quad (5.12)$$

This can be seen as a generic writing of the reference trajectories for these Euler-Lagrange energy based schemes.

The desired state (5.12) are parametrised in terms of the desired torque $\tau_d(t)$ and the auxiliary input variable $\omega_s(t)$. Now a set of reference trajectories are established in terms of the desired states of the motor x_d . This property will be very helpful when, in Chapter 7, a control law will be used to “shape” the energy along a given desired torque trajectory. The slip frequency represents the degree of freedom to use in the energy optimization done in Chapter 6.

Clearly, there is a singularity problem in (5.12) for $\tau_d(t) = 0$ or $\omega_s(t) = 0$. Nevertheless, there are two ways to surmount this problem; (i) either is an assumption introduced on τ_d and ω_s , or (ii), as will be shown in Section 5.2, is the slip frequency chosen in a special way. The latter overcomes the problem in question but prevents an energy optimization.

Under the assumptions that

$$\lim_{\tau_d \rightarrow 0} \sqrt{\tau_d / \omega_s} < \infty \quad (5.13)$$

$$\lim_{\tau_d \rightarrow 0} \frac{d}{dt} \left[\sqrt{\tau_d / \omega_s} \right] < \infty \quad (5.14)$$

the desired state (5.12) fulfills the torque tracking objective and the field orientation (5.6) is also obtained. Moreover are the dynamical motor equations (5.2) assured for all $\omega_s(t)$ with bounded input signals u .

The boundedness of $\sqrt{\tau_d / \omega_s}$ and $\frac{d}{dt} \left[\sqrt{\tau_d / \omega_s} \right]$ is guaranteed by assumptions (5.13) - (5.14). They, in turn, answer for the boundedness of x_d which, with the smoothness of τ_d and ω_s , imply that \dot{x}_d is bounded. Furthermore, the boundedness of x_d and \dot{x}_d implies the boundedness of $[u_{d1} \ u_{d2}]^T$ given by (5.3).

¹We will drop the time argument from now on. It will be used only when necessary.

5.2 Constant Rotor Flux Model

Under the same considerations as above, the assumptions (5.13) and (5.14) can be relaxed by choosing

$$\omega_s = \alpha \tau_d \quad (5.15)$$

whereby the singularity of (5.12) is removed. The positive constant α determines the level of the d component of the rotor flux.

Putting (5.15) into (5.12) gives us

$$\begin{aligned} x_{d1} &= -\frac{1}{L_{sr}} \sqrt{\frac{R_r}{v\alpha}} \\ x_{d2} &= -\frac{L_r}{L_{sr}} \sqrt{\frac{\alpha}{R_r v}} \tau_d \\ x_{d3} &= 0 \\ x_{d4} &= \sqrt{\frac{\alpha}{R_r v}} \tau_d \end{aligned} \quad (5.16)$$

which are bounded since τ_d is \mathcal{L}_∞ .

This selection does indeed remove the singularity but leaves no degree of freedom to use in transient optimization.

One particular choice of the slip frequency

$$\omega_s = \alpha_0 \tau_d \quad ; \quad \alpha_0 = \frac{R_r}{v \phi_{ref}^2} \quad (5.17)$$

corresponds to the solution proposed in [13]. The reference flux ϕ_{ref} , which determines the flux level of the motor is usually fixed as to attain the nominal rate of the motor flux. Smaller values of ϕ_{ref} can be used which naturally imply smaller magnetic flux in the machine.

Chapter 6

Optimization

In this Chapter we will, using the structure developed in Chapter 5, study the problem of finding the solution which minimizes the total desired magnetic energy of the motor

$$\mathcal{H}(\mathbf{x}_d) = \frac{1}{2} \mathbf{x}_d^T D \mathbf{x}_d \quad (6.1)$$

for a given time interval $t_0 \leq t \leq t_f$.

The main interest in minimizing the magnetic energy concerns the efficiency aspects of the motor. Such optimization criterion maximizes the power factor of the motor and is a good compromise in terms of power losses [14, 15].

The desired energy function (6.1) can be written in terms of the desired torque τ_d and the slip frequency ω_s . Putting (5.12) into (6.1) and after some manipulations, we obtain

$$\begin{aligned} \mathcal{H}(\mathbf{x}_d) &= \mathcal{H}(\tau_d, \dot{\tau}_d, \omega_s, \dot{\omega}_s) \\ &= c \left(\frac{\tau_d}{\omega_s} \frac{R_r^2}{L_s^2 \sigma} + \tau_d \omega_s + \frac{R_r}{L_r} \frac{d[\tau_d]}{dt} + \left\{ \frac{d}{dt} \left[\sqrt{\frac{\tau_d}{\omega_s}} \right] \right\}^2 \right) \end{aligned} \quad (6.2)$$

with

$$c = \frac{L_r \sigma}{2v R_r (1 - \sigma)} \quad ; \quad \sigma = 1 - \frac{L_{sr}^2}{L_s L_r}$$

Using assumption A.2, i.e. the knowledge of τ_d and $\dot{\tau}_d$, we have the possibility to rewrite (6.2) as

$$\mathcal{H}(\tau_d, \dot{\tau}_d, \omega_s, \dot{\omega}_s) = \mathcal{H}(t, \omega_s, \dot{\omega}_s)$$

6.1 Problem Formulation

This part will extend the studies done in [4, 14]. The minimization was there performed directly on the energy function (6.1), but since we have an obvious dependency between ω_s and $\dot{\omega}_s$ in our expression for the energy (6.2) it will not be possible to do so here.

In order to derive the optimal slip frequency, ω_s^* , we are obliged to examine an integral of the energy function (6.2) for the given time interval. This leads us, without any option, to the calculus of variations [5].

Furthermore, the energy equation (6.2) suggests us a change of coordinates

$$y = \sqrt{\frac{\tau_d}{\omega_s}} \quad (6.3)$$

such that it can be written as:

$$\mathcal{G}(t, y, \dot{y}) = c(w_0^2 y^2 + \frac{\tau_d^2(t)}{y^2} + w_0 \sqrt{\sigma} \frac{d}{dt} \{y^2\} + \dot{y}^2) \quad (6.4)$$

We will now pose the problem as:

Find the function $y^ = y(t)$, continuously differentiable for $t_0 \leq t \leq t_f$, satisfying the boundary conditions*

$$y(t_0) = \sqrt{\frac{\tau_d(t_0)}{\omega_0}} \quad ; \quad y(t_f) = \sqrt{\frac{\tau_d(t_f)}{\omega_0}} \quad (6.5)$$

for which the functional

$$J[y] = \int_{t_0}^{t_f} \mathcal{G}(t, y, \dot{y}) dt = \int_{t_0}^{t_f} c(w_0^2 y^2 + \frac{\tau_d^2(t)}{y^2} + w_0 \sqrt{\sigma} \frac{d}{dt} \{y^2\} + \dot{y}^2) dt \quad (6.6)$$

has a weak extremum.

The boundary conditions (6.5) correspond to optimum energy steady-states of the motor (see [4, 14]), i.e.

$$\omega_0 = \arg \min_{\omega_s} x_d^T D x_d \quad \text{subject to} \quad \dot{x}_d = 0 \quad (6.7)$$

which has the solution

$$\omega_0 = \frac{R_r}{L_r \sqrt{\sigma}} \quad (6.8)$$

The condition in (6.7) implies, as we see by simply inspecting (5.12), that

$$\begin{aligned} \dot{\tau}_d(t_0) &= \dot{\tau}_d(t_f) = 0 \\ \dot{\omega}_s(t_0) &= \dot{\omega}_s(t_f) = 0 \end{aligned}$$

Notice that the integral

$$\int_{t_0}^{t_f} w_0 \sqrt{\sigma} \frac{d}{dt} \{y^2\} = \sqrt{\sigma} (\tau(t_f)^2 - \tau(t_0)^2) \quad (6.9)$$

is invariant with respect to y and therefore so for ω_s , too. This suggests a reformulation of the weak extremum problem (6.5)-(6.6) reading:

Find $y^* = y(t)$ continuously differentiable for $t_0 \leq t \leq t_f$ satisfying the boundary conditions (6.5) for which the functional

$$J[y] = \int_{t_0}^{t_f} \mathcal{F}(t, y, \dot{y}) dt = \int_{t_0}^{t_f} c(\omega_0^2 y^2 + \frac{\tau_d^2}{y^2} + \dot{y}^2) dt \quad (6.10)$$

has a weak extremum.

The solution of this problem gives the extremum in terms of the ratio $y^* = \sqrt{\frac{\tau_d}{\omega_0}}$. Since both y^* and τ_d are smooth, the optimum function ω_0^* is obtained directly from y^* .

6.2 The Existence of Solution

According to the theory of calculus of variation [5], the sufficient conditions for the curve $y^* = y(t)$ to be an extremum of (6.10) are the following three:

1. y^* shall satisfy the Euler's equation, i.e.,

$$\frac{\partial \mathcal{F}}{\partial y} - \frac{d}{dt} \left\{ \frac{\partial \mathcal{F}}{\partial \dot{y}} \right\} = 0 \quad (6.11)$$

to guarantee the existence of a solution.

2. Along the curve $y^* = y(t)$ shall

$$P(t) = \frac{1}{2} \frac{\partial^2 \mathcal{F}}{\partial \dot{y}^2} > 0 \quad (6.12)$$

to assure that y^* corresponds to a minimum. This stems from the criterion of nonnegativity of the second variation.

3. The interval $[t_0, t_f]$ contains no points conjugate to the point t_0 , in other words, the quadratic functional

$$\int_{t_0}^{t_f} (P h^2 + Q \dot{h}^2) dt \quad (6.13)$$

where

$$P(t) > 0 \quad ; \quad Q(t) = \frac{1}{2} \left(\frac{\partial^2 \mathcal{F}}{\partial y^2} - \frac{d}{dt} \left\{ \frac{\partial^2 \mathcal{F}}{\partial y \partial \dot{y}} \right\} \right) \quad (6.14)$$

is nonnegative for all arbitrary functions $h(t)$, smooth in the interval $[t_0, t_f]$, such that $h(t_0) = h(t_f) = 0$. If there should be conjugate points in the interval, the solution is not a unique minimum since there are more than one policy which gives the same result.

It is easily seen that our function \mathcal{F} from (6.10) matches the two last conditions since

$$P(t) = c > 0 \quad ; \quad Q(t) = c \left(\omega_0^2 + 3 \frac{\tau_d^2}{y^4} \right) > 0 \quad \forall t \in [t_0, t_f] \quad (6.15)$$

Condition 1 implies that if there exist a solution then this should satisfy the Euler equation (6.11), which in turn, represents a second order nonlinear differential equation. In our case can (6.11) be written as

$$\ddot{y}y^3 - \omega_0^2 y^4 = -\tau_d^2 \quad (6.16)$$

to which there is no explicit solution expressed as a function of τ_d . Therefore, we will try to find a numerical solution to our problem for certain specified torque paths.

6.3 Dynamic Programming

To work with second order nonlinear differential equations may involve some problems. Only in rare cases can an explicit analytic solution be found in terms of the standard functions of analysis. However, the well known dynamic programming method, invented by Bellman [2], lets us avoid this difficulty and directly attack the functional (6.10). This numerical method gives us unfortunately a posterior solution to the problem and can thus not be applied for an on-line implementation.

Dynamic programming is essentially a clever way of examining all the candidates for an optimal control law. It is based on the Principle of Optimality:

An optimal policy has the property that whatever the initial state and initial decision are, the remaining decisions must constitute an optimal policy with regard to the state resulting from the first decision.

To implement the additive cost functional (6.10) we need to quantize the slip frequency, and it seems reasonable to do so in a region around the steady-state solution ω_0 . We assume that the discretization procedure is shown to be stable in the sense that it yields a suboptimal solution which is close to the continuous policy. Discretizing the cost function J leads to

$$J_k(y) = \sum_{i=k}^{N-1} F(i\Delta, y_i, z_i) \Delta$$

where Δ denotes the time increment and the derivative is approximated by

$$z_i = \frac{y_{i+1} - y_i}{\Delta}$$

F is defined as in (6.2) and $y = \{y_i\}$ signifies the control sequence, i.e. the slip frequency.

The minimization will be performed from the end to the beginning and therefore we introduce a "until-now" cost

$$f_k(y_k) = \min_{\{y_i\}} J_k(y) \quad (6.17)$$

This corresponds to the minimal cost that will take the system from the point y_k at time $k\Delta$ to the final state. Using the principle of optimality to develop (6.17) results in

$$f_k(y_k) = \min_{z_k} [F(k\Delta, y_k, z_k) \Delta + f_{k+1}(y_k + z_k \Delta)] \quad (6.18)$$

The expression (6.18) reveals the computational complexity, which Bellman called the “curse of dimensionality”, of this algorithm. The primary limitation of dynamic programming is on the computational time and memory storage required for high resolution. Taking, for example, 50 discretization points on the slip frequency axis and 40 on the time axis results in a 40×50 grid. For each of these points, the function F has to be evaluated and a minimization performed. However, once a search space has been defined the implemented procedure is as follows:

1. For each possible value of y_{N-1} , calculate the cost to go to the final state and store them.
2. For each following step and each accessible y_i , find the policy, which transfer the present state to the y_{i+1} that gives the minimum cost. Store this and the hitherto cost (6.18) for each value of y_i .
3. When the calculation is terminated the initial condition indicates the optimal policy.

One way to speed up this algorithm is to first calculate a low- resolution solution and then center the next evaluation around this. Several iterations may be done to get a good solution.

6.4 Numerical Solution

In this section will we apply the dynamic programming to three torque references. These has to be smooth enough to ensure the initial and the final conditions posed in the problem formulation.

The desired torques considered are of the form

$$\tau_d(t) = 10 + \alpha \left(1 - e^{-\beta t^2}\right)^3 \quad (6.19)$$

Our choice, (6.19), has first and second derivative equal to zero at the initial and the final points. We will study three cases with the following values on the change of amplitude and the time constant

Case	α (Nm)	β (s^{-2})
A	5	100
B	10	100
C	10	500

Since the motor parameters appear in the energy function, the solutions presented are restricted to this motor but they express the general form for the considered torque references.

The resistances and inductances of the motor used in the calculations are

Stator resistance	R_s	0.687	Ω
Rotor resistance	R_r	0.842	Ω
Stator inductance	L_s	0.084	H
Rotor inductance	L_r	0.085	H
Mutual inductance	L_{sr}	0.081	H

The first two trajectories corresponds to a torque change within 0.2 s and the last one is approximately in the order of 0.1 s. This can be seen in Fig. 6.1. The implementation of dynamic programming algorithm was done using MATLAB.

All the optimal policies, in Fig 6.2, oscillate around the steady-state value which is equal to the boundary conditions. Even if the change seems big for case C, does it not exceed a 10 % boundary. Of course will a faster torque change imply larger deviations. The peaks of the slip frequency solution grows with the torque change and they also do so if the change is faster.

Since the calculation is not done on-line, it has to be precalculated. This means that a policy has to be stocked for each type of torque form which can occur in the system requirements, which is almost an unrealistic task. This justifies the choice of a constant slip frequency, $\omega_s = \omega_0$, as we will use in the rest of this study.

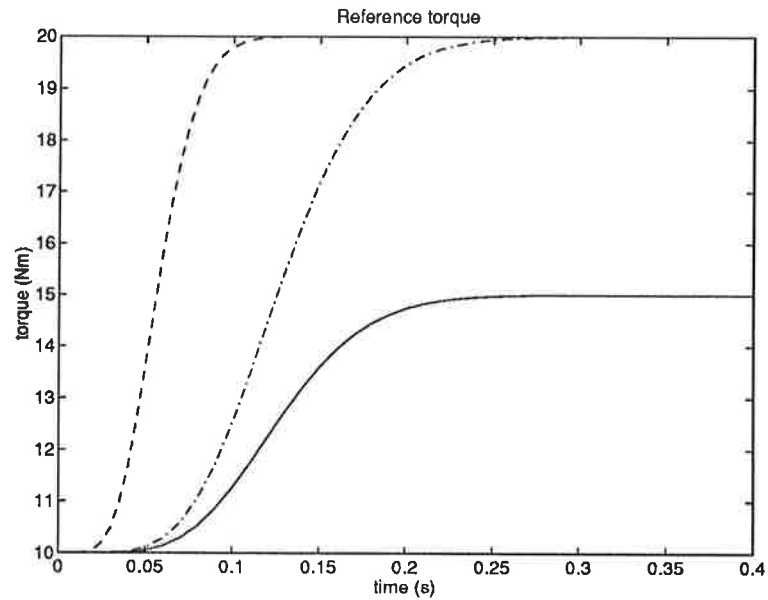


Figure 6.1: The reference torques. A solid, B dash-dotted and C dashed.

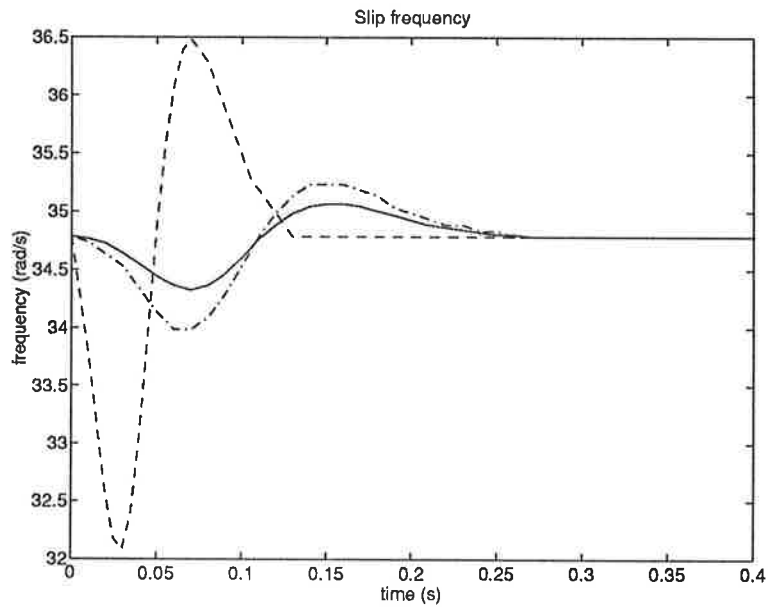


Figure 6.2: The optimal policies calculated using dynamic programming. A solid, B dash-dotted and C dashed.

Chapter 7

Control

In the previous chapters we were able to establish reference states which, for desired torque trajectories such that $\tau_{min} < |\tau_d| < \tau_N$, are optimal in the sense of energy. They are also formulated as functions of the desired output for all time $t_0 \leq t \leq t_f$ so that the desired torque is ensured.

When the torque reference value $|\tau_d|$ is outside the interval $[\tau_{min}, \tau_N]$, we shall switch to an alternative reference trajectory as given in Section 5.2. This will remove the singularity problem for $\tau_d = 0$, and also, when the reference torque value is larger than the machine's rated value, limitate the d component of the desired rotor flux

$$\phi_r^d = L_{sr}x_{d1} + L_r x_{d3} \quad (7.1)$$

to its nominal value, and thus eliminate saturation problems.

The problem to be studied now is that of torque tracking under minimum energy consumption. This correspond to make $x \rightarrow x_d$ of (5.12) for $\tau \in [\tau_{min}, \tau_N]$, or in other words, to render invariant the manifold

$$\xi(x, t) = x - x_d(t) = 0 \quad (7.2)$$

7.1 Stability Analysis

We shall now construct a feedback control to perform minimum energy torque tracking, using the approach proposed in [3, 13] for Euler-Lagrange based systems.

First, let the error signal be defined by

$$e = x - x_d \quad (7.3)$$

Consider the motor system (3.1)-(3.2) and the mechanical system (3.3). Let the control law for the motor system be given in terms of the feedforward term, u_d , from

(5.3), and a linear static feedback

$$\begin{aligned} \begin{bmatrix} u_1 \\ u_2 \end{bmatrix} &= u_d - K(x - x_d) \\ &= M^+ \{ D\dot{x}_d + [N(u_3, \dot{q}) + R]x_d - n(x_d)\dot{q} \} - K(x - x_d) \\ u_3 &= v\dot{q} + \omega_s \end{aligned} \quad (7.4)$$

where x_d is given by (5.12) and the (2×4) feedback matrix defined as

$$K \stackrel{def}{=} \begin{bmatrix} K_1 & K_2 \end{bmatrix} ; \quad K_i \stackrel{def}{=} \begin{bmatrix} k_{i1} & k_{i2} \\ k_{i3} & k_{i4} \end{bmatrix} \quad (7.5)$$

Then the error equation for the motor, obtained by inserting (7.4) into (3.1), is

$$D\dot{e} + [N(u_3, \dot{q}) + R + MK]e - n^T(e)\dot{q} = 0 \quad (7.6)$$

Let also, the desired torque be given by the feedback law

$$\tau_d = J\ddot{q}_r + b\dot{q}_r + \tau_L - k_v(\dot{q} - \dot{q}_r) \quad (7.7)$$

where \dot{q}_r and \ddot{q}_r are reference speed and acceleration, respectively. They are both smooth and bounded. The torque regulation problem has, with the last term in (7.7), been transformed into a speed-regulation problem.

Constructing the mechanical error equation from (3.3) and (7.7), with the errors given by

$$\tilde{q} := \dot{q} - \dot{q}_r ; \quad \ddot{\tilde{q}} := \ddot{q} - \ddot{q}_r$$

results in

$$J\ddot{\tilde{q}} + b\dot{\tilde{q}} = \tau(x) - \tau_d \quad (7.8)$$

Developing the right hand side of (7.8), using (3.2) and the property of (5.12), brings forth

$$\begin{aligned} \tau(x) - \tau_d &= \tau(x) - \tau(x_d) \\ &= \tau(e) - vL_{sr} \begin{bmatrix} x_{d4} & -x_{d3} & -x_{d2} & x_{d1} \end{bmatrix} e \end{aligned}$$

This expression is a key to the stability analysis below, since the second right hand term is linear in e .

Introducing the following state vector

$$z = \begin{bmatrix} e_1 & e_2 & e_3 & e_4 & \dot{\tilde{q}} \end{bmatrix} \quad (7.9)$$

permits a full state representation of the two subsystems. The new error system can be written as

$$\mathcal{D}\dot{z} + [\mathcal{N} + \mathcal{R}]z = 0 \quad (7.10)$$

with the 5×5 matrices defined as

$$\mathcal{D} \stackrel{def}{=} \begin{bmatrix} D & 0_{4 \times 1} \\ 0_{1 \times 4} & J \end{bmatrix}$$

$$\mathcal{N} \stackrel{def}{=} \begin{bmatrix} N(u_3, \dot{q}) & -n(e) \\ n^T(e) & 0 \end{bmatrix} ; \quad \mathcal{N}^T = -\mathcal{N}$$

$$\mathcal{R} \stackrel{def}{=} \begin{bmatrix} R_s \mathcal{I}_2 + K_1 & K_2 & 0_{2 \times 1} \\ 0_{2 \times 2} & R_r \mathcal{I}_2 & 0_{2 \times 1} \\ v L_{sr} x_{d4} & -v L_{sr} x_{d3} & -v L_{sr} x_{d2} & v L_{sr} x_{d1} & b + k_v \end{bmatrix}$$

In view of (7.10) and consistently with the physical constraints of the original systems (3.1) and (3.3), we introduce the Lyapunov function

$$V(z) \stackrel{def}{=} \frac{1}{2} z^T \mathcal{D} z \quad (7.11)$$

This can be regarded as the energy of the error system. Evaluating the time derivative of (7.11) along the trajectories of (7.10) results in

$$\begin{aligned} \dot{V}(z) &= z^T \mathcal{D} \dot{z} \\ &= -z^T [\mathcal{N} + \mathcal{R}] z \\ &= -z^T \mathcal{R} z \end{aligned} \quad (7.12)$$

since \mathcal{N} is skew symmetric. If we can assure that \mathcal{R} is positive definite (and symmetric) then the prescribed reference trajectory is globally asymptotically stable. Calculating the eigenvalues of \mathcal{R} gives

$$\begin{aligned} \lambda_{1,2} &= R_s + \frac{k_{11} + k_{14}}{2} \\ &\pm \sqrt{\left(R_s + \frac{k_{11} + k_{14}}{2}\right)^2 + k_{12}k_{13} - (R_s + k_{11})(R_s + k_{14})} \end{aligned} \quad (7.13)$$

$$\lambda_{3,4} = R_r ; \quad \lambda_5 = b + k_v$$

Evaluating (7.13) reveals the following condition to ensure positive definiteness

$$k_{13}k_{12} - (k_{11} + R_s)(k_{14} + R_s) < 0 \quad (7.14)$$

Hence, in the sense of stability we can conclude that we don't need full state measurement since the criterion is independent of the feedback matrix K_2 . Moreover, even K_1 may be set to zero, if we have no demands for faster convergence. Otherwise, a good and simple form of K_1 is the diagonal one, which will be used in the sequel.

We can now conclude that the closed loop system is globally convergent, i.e., $\tau \rightarrow \tau_d$ as $t \rightarrow \infty$ with internal stability.

Since the rotor currents, x_3 and x_4 , are not available for direct measurement, an important conclusion here is that we do not need an observer in the implementation of our control law, if $K_2 = 0$. This result was also recently obtained by Espinosa and Ortega. This relaxes assumption A.1 to a more realistic one.

7.2 The Control Law

The discussion above is independent of the choice of slip frequency. In order to avoid singularity and saturation problems we will switch the slip frequency when needed. This will be done at two torque levels; τ_N , which is called the nominal torque, and τ_{min} , which is the minimum torque to be applied by the minimum energy control algorithm. The latter is used to overcome the singularity. Using (5.16), we define the auxiliary variable as

$$\omega_s = \begin{cases} \omega_s^* & \text{for } \tau_{min} < |\tau_d| < \tau_N \\ \alpha_{min}\tau_d & \text{for } |\tau_d| < \tau_{min} \\ \alpha_{max}\tau_d & \text{for } |\tau_d| > \tau_N \end{cases} \quad (7.15)$$

with

$$\alpha_{min} = \frac{R_r}{v\phi_{min}^2} \quad ; \quad \alpha_{max} = \frac{R_r}{v\phi_{max}^2} \quad (7.16)$$

Where ϕ_{max} corresponds to the rated flux and ϕ_{min} to the minimum admissible flux in the machine. These are to be established experimentally. Above, τ_N is the nominal torque and τ_{min} is the minimum torque. The latter is used to overcome the singularity. The last parameter to select in the torque regulation design is the static feedback matrix, which is chosen as

$$K \stackrel{def}{=} \begin{bmatrix} k_1 & 0 & 0 & 0 \\ 0 & k_2 & 0 & 0 \end{bmatrix} \quad (7.17)$$

The control signals are then described by (7.4).

The propagation through the control system of all signals can be seen in Fig 7.1. The desired torque enters the system from left and generates the slip frequency and the state reference. The latter is used both in the feedforward part and in the state error feedback. To the right we find the process to be controlled; the motor and the mechanical system, between which the resulting torque is found. All equation used to generate a new signal are noted in the boxes.

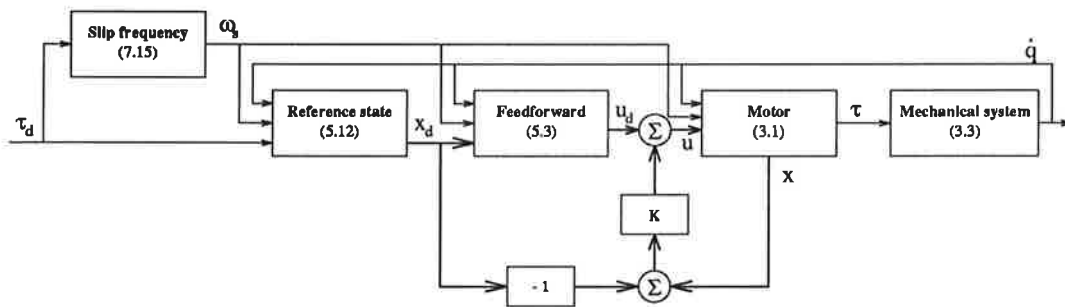


Figure 7.1: The control scheme.

Chapter 8

Simulation Results

In this chapter will we simulate the induction motor with one of the reference torques from Section 6.3, namely *Case B*. All the simulations are done using the software SIMNON [16]. The objective is to verify that we have good convergence with the controller proposed in Section 7.2, and that the torque tracking objective is fulfilled. We shall also do an energy comparison between our control scheme and the off-line calculated optimal policy from Section 6.3.

Numerical values of the induction motor are enclosed in Section 6.4 for which the mechanical system and the controller, from Section 7.2, used in the simulations are described by

Shaft inertia	J	0.03	$kg\ m^2$
Motor damping	b	0.1	$kg\ m^2/s$
Pole pairs	v	1	
Feedback gain	k_1	1	V/A
Feedback gain	k_2	1	V/A

The reference trajectory is shown in Fig 8.1 with the output torque. The motor is initially at stand still with zero initial conditions and the reference value is then 10 Nm.

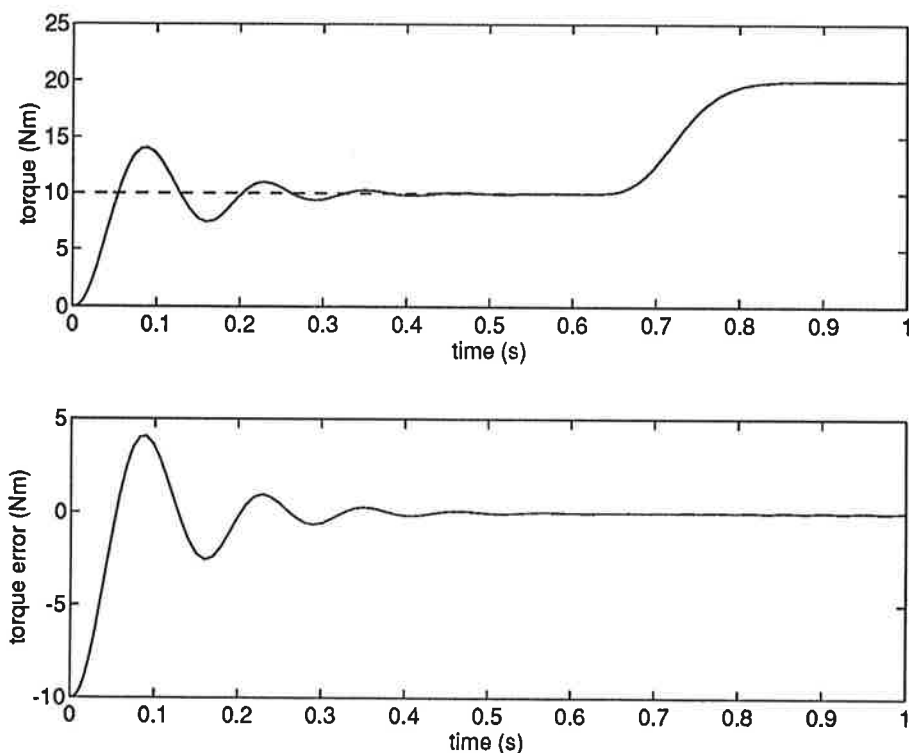


Figure 8.1: The reference and output torque on top and the torque tracking error below.

The overshoot for the torque during control is fully acceptable. Other choices and structures of the K matrix would improve the behavior of the system, but such study will be omitted here.

At time 0.6 s, when the the states have converged to the desired ones, a torque change is done of the form of (6.19). The torque tracking error has a small transient behavior, and indicates that once we have obtained the reference trajectory, we will, for a sufficiently smooth torque reference, stay in this path.

Fig. 8.2 shows the current transients and the fluxes, which are linear combinations of the currents, are plotted in Fig. 8.3. From the maximum absolute values in the last figure, we can conclude that there is no iron saturation since the magnetic flux limit of the machine is not reached. The waveforms have a initial transients, but are completely satisfying.

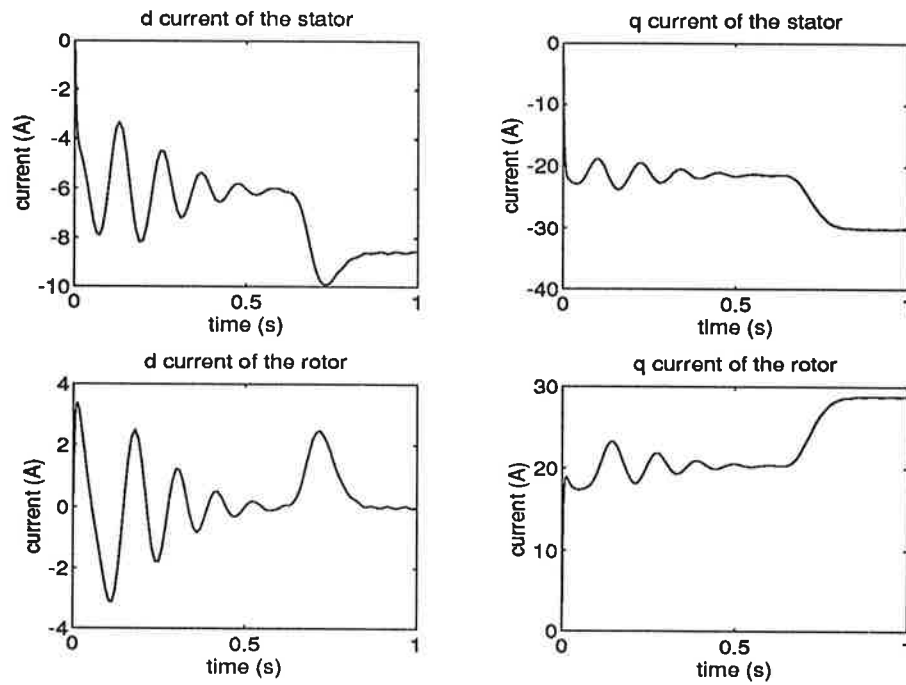


Figure 8.2: The currents in the motor during torque tracking.

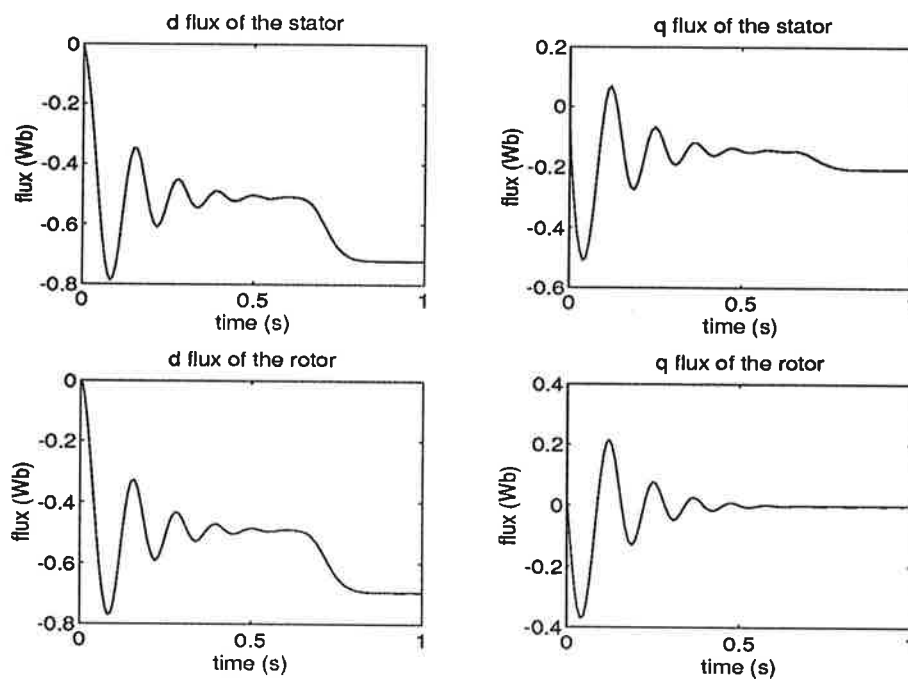


Figure 8.3: The fluxes in the motor during torque tracking.

Our main interest has been the magnetic energy, \mathcal{H} . Fig. 8.4 shows the energy of the motor with the control scheme presented in Section 7.2.

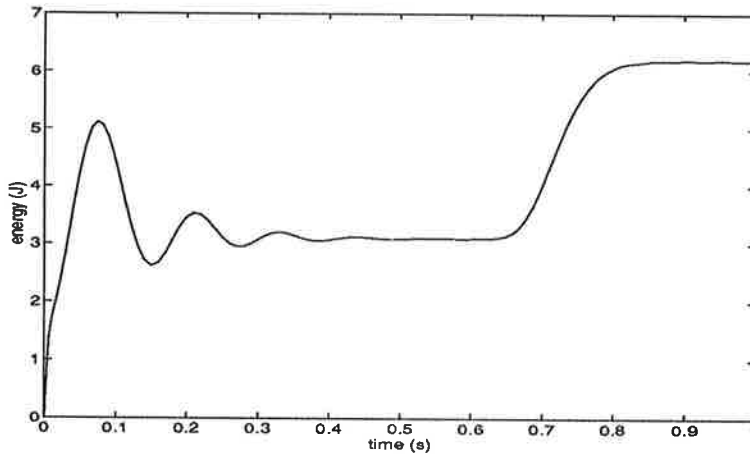


Figure 8.4: The magnetic energy, \mathcal{H} , stored in the induction motor.

The most astonishing fact is that it does not differ much from the energy in a system where the optimal slip frequency (derived in Section 6.4) has been used as an input. The instantaneous difference is shown in Fig. 8.5.

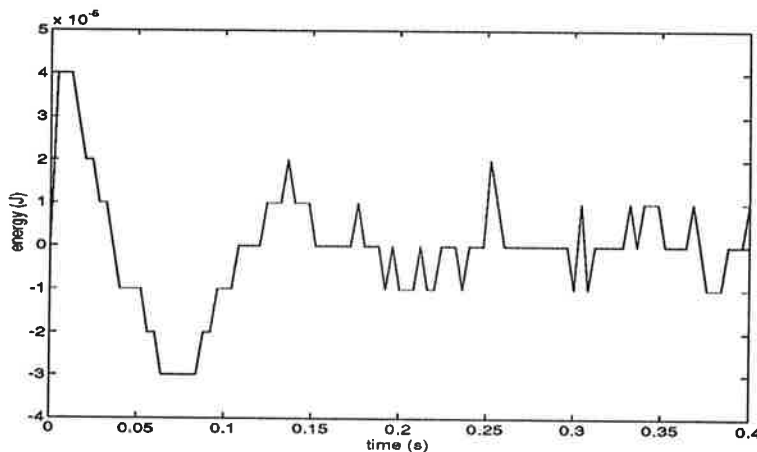


Figure 8.5: The difference in magnetic energy between the control law with constant slip frequency and the one with the optimal off-line policy (presented as $\mathcal{H}_{sub} - \mathcal{H}_{opt}$).

Even if there is a tiny difference, this validates our suboptimal choice of ω_0 as the slip frequency, which was done in Section 7.2. Suppose a faster change of torque would occur. Then there would be a larger and more visible difference in energy storage.

The discrete characteristics of the waveform is due to the time quantization used to obtain the numerical solution. The largest difference occurs just before the torque

starts to increase and the next maximum just before the levelling (compare with Fig. 8.1 starting from $t = 0.6$ s until the end).

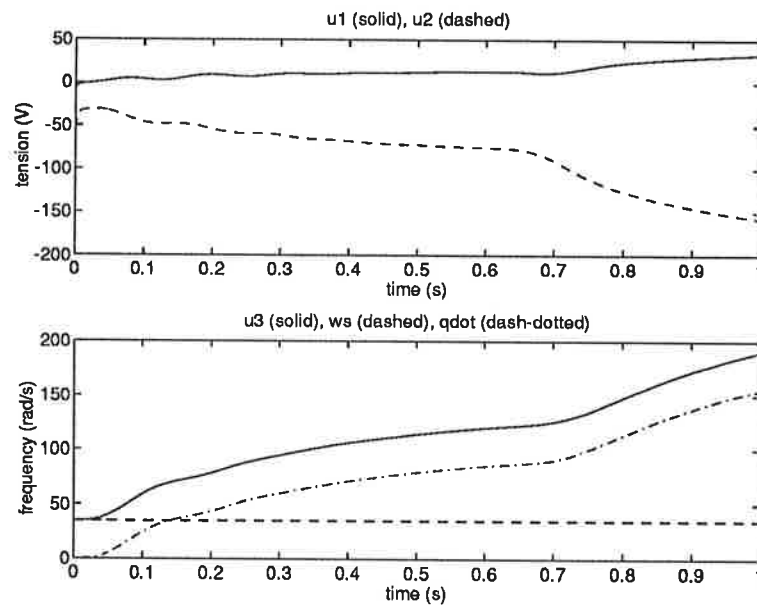


Figure 8.6: The control variables, the slip frequency and the rotor speed.

Another important aspect is the control variables fed to the motor. The stator voltages are presented in Fig. 8.6 where all the frequency quantities are shown in the lower half. The voltages rise with the speed. The latter is bounded and therefore will the input variables also remain bounded.

Chapter 9

Conclusion

This study presents a nonlinear control law which stabilizes the induction motor and almost minimizes the magnetic energy. The Lyapunov-stability analysis showed a global convergence to the desired trajectory using a simple static feedback matrix. Simulation has shown that the proposed control design yields a good behaviour even under energy optimization. In any case, for desired torques smaller than the machine's rated value, the present operation scheme is more efficient than field-oriented like schemes which constantly operate at maximum rotor flux. The improvement of efficiency depends on the specific operation regions. In order to really compare these two concepts I propose that a study of them with simulations and/or practical tests.

The minimum energy approach are presently subject to experimental evaluation [15]. There is also a new investigation in the direction of minimizing the energy and the losses in the machine

$$J = \mathcal{H} + \alpha P_{loss}$$

If τ_d should be unknown, which is likely, and regarding the variation of the rotor resistance, R_r , a future enlargement of this design concept with an adaptive scheme should be considered.

The induction motor, using this type of control schemes, offer a very promising alternative for applications like the electrical vehicles, which are to come in the near future in California. Other domains are the industrial field and trains, which have long-term steady-state running cycles. Even in robotics there is a use. Some great advantages of the induction motor is that it has no failure-prone brushes and it don't need maintenance very often.

Appendix A

Notations

i_s^d	x_1	d component of the stator current
i_s^q	x_2	q component of the stator current
i_r^d	x_3	d component of the rotor current
i_r^q	x_4	q component of the rotor current
	$x_{d1} \cdots x_{d4}$	Reference states
V_s^d	u_1	d component of the stator voltage
V_s^q	u_2	q component of the stator voltage
	u_{d1}, u_{d2}	Stator reference voltages
ω_a	u_3	Primary frequency
	ω_s	Slip frequency
	\dot{q}	Mechanical angular speed
	\dot{q}_r	Reference angular speed
	τ	Output torque
	τ_d	Torque reference
	τ_L	Load torque
	ϕ_s^d	d component of the stator flux
	ϕ_s^q	q component of the stator flux
	ϕ_r^d	d component of the rotor flux
	ϕ_r^q	q component of the rotor flux
	R_s	Stator resistance
	R_r	Rotor resistance
	L_s	Stator inductance
	L_r	Rotor inductance
	L_{sr}	Mutual inductance
	J	Rotor inertia
	b	Motor damping
	v	Number of pole pairs



Bibliography

- [1] F. Blaschke, "Principle of field orientation as applied to the new Transvector closed-loop control system for rotating field machines", *Siemens Rev.*, p.217, 1971.
- [2] R. Bellman and S. Dreyfus, **Applied Dynamic Programming**, Princeton Univ. Press, Princeton, New Jersey, 1962.
- [3] C. Canudas, R. Ortega and S. I. Seleme, "Robot motion control using induction motor drives", *ICRA '93*, May 2-7 Atlanta - USA (Submitted also to *Trans. on Robotics and Aut.*), 1992.
- [4] C. Canudas de Wit and S. I. Seleme, "Lyapunov based torque control design for induction motors: the minimum energy approach", *IFAC World Congress93*, Sydney, 18-23 July, Australia, 1992.
- [5] I. M. Gelfand and S. V. Fomin, **Calculus of Variations**, Prentice-Hall Inc., New Jersey, 1963.
- [6] R. Johansson, "Quadratic optimization of motion coordination and control", *Proc. IEEE ICRA*, pp.1204-1209, 1990.
- [7] R. Johansson, "Quadratic optimization of motion coordination and control", *IEEE Trans. on Aut. Control*, vol. 35, No. 11, pp.1197-1208, 1990.
- [8] W. Leonhard, "Microcomputer control of high-performance dynamic AC drives: A survey", *Automatica*, Vol. 22, No.1, pp. 1-19,1986.
- [9] R. D. Lorenz and S. M. Yang, "Efficiency-optimized flux trajectories for closed-cycle operation of field-orientation induction machine drives", *IEEE Trans. Ind. Appl.*, Vol. IA-28, No. 3, pp. 574-580, 1992.
- [10] R. D. Lorenz and S. M. Yang, "AC induction servo sizing for motion control applications via loss minimizing real-time flux control", *IEEE Trans. Ind. Appl.*, Vol. IA-28, No. 3, pp. 589-593, 1992.
- [11] R. Ortega and G. Espinosa, "A Controller Design Methodology for Systems with Physical Structures: Application to Induction Motors", *Proc. IEEE CDC*, Brighton, UK, Dec. 1991.

- [12] R. Ortega and G. Espinosa, "Torque regulation of induction motors", *Automatica*, Vol. 29, No. 3, pp. 621-633, 1993.
- [13] R. Ortega, C. Canudas and S. I. Seleme, "Nonlinear control of induction motors: torque tracking with unknown load disturbance", *Proc. ACC*, Chicago, USA, June 1992. (Also to appear in *IEEE Trans. Aut. Cont.*), 1992.
- [14] S. I. Seleme and C. Canudas de Wit, "Minimum energy operation conditions of induction motors under torque control", *Workshop on Motion Control for Intelligent Automation'92*, Perugia, 27-29 October, Italy, vol.1, pp. 127-133, 1992.
- [15] S. I. Seleme, E. Mendes, C. Canudas de Wit and A. Razek, "Experimental validation of the minimum energy approach for induction motor control", to be presented at *IEEE / SMC'93 Conference*, Le Touquet, France, October 17-20, 1993.
- [16] SSPA, **Simnon User's Guide for MS-DOS Computers**, Department of Automatic Control, Lund Institute of Technology, Sweden, 1990.